Distributing test cases more evenly in adaptive random testing

Distributing Test Cases More Evenly in Adaptive Random Testing*

Tsong Yueh Chen, Fei-Ching Kuo, Huai Liu†

Faculty of Information and Communication Technologies

Swinburne University of Technology

John Street, Hawthorn, Victoria 3122, Australia.

Abstract

Adaptive Random Testing (ART) has recently been proposed to enhance the failure-detection capability of *Random Testing*. In ART, test cases are not only randomly generated, but also evenly spread over the input domain. Various ART algorithms have been developed to evenly spread test cases in different ways. Previous studies have shown that some ART algorithms prefer to select test cases from the edge part of the input domain rather than from the centre part, that is, inputs do not have equal chance to be selected as test cases. Since we do not know where the failure-causing inputs are prior to testing, it is not desirable for inputs to have different chances of being selected as test cases. Therefore, in this paper, we investigate how to enhance some

*A preliminary version of this paper was presented at the 18th Australian Software Engineering Conference (ASWEC 2007) (Chen et al., 2007b).

†Corresponding author. Tel.: +61 3 9214 5276; fax: +61 3 9819 0823.

E-mail addresses: tchen@ict.swin.edu.au (T.Y. Chen), dkuo@ict.swin.edu.au (F.-C. Kuo), hliu@ict.swin.edu.au (H. Liu).

ART algorithms by offsetting the edge preference, and propose a new family of ART algorithms. A series of simulations have been conducted and it is shown that these new algorithms not only select test cases more evenly, but also have better failure detection capabilities.

Keywords: Software Quality, Software Testing, Random Testing, Adaptive Random Testing, Test Case Distribution.

1 Introduction

Software testing is a major approach to software quality assurance. There exist many testing methods which actively select inputs for testing (namely *test cases*) in order to effectively detect software failures. *Random Testing* (RT) is a basic software testing method, which simply selects test cases in a random manner from the set of all possible inputs (namely the *input domain*) (Hamlet, 2002; Myers, 2004). RT has many advantages as a software testing method. For example, it can automatically generate a large number of test cases at low cost, and the test case generation is not influenced by any human bias. What is more, its "randomness" may help reveal failures which cannot be detected by deterministic approaches (such as domain testing (White and Cohen, 1980), data flow testing (Laski and Korel, 1983), and branch testing (Myers, 2004)). Because of these advantages, RT has been successfully applied to detect software failures in industry, such as the testing of UNIX utilities (Miller et al., 1990, 1995), SQL database systems (Slutz, 1998), Windows NT applications (Forrester and Miller, 2000), Java Just-In-Time compilers (Yoshikawa et al., 2003), and embedded software systems (Regehr, 2005). However, some researchers (Myers, 2004) argued that RT may be the "least effective" testing method because it uses little or no information about the program under test.

A number of studies (Ammann and Knight, 1988; Finelli, 1991; Bishop, 1993) have independently shown a common characteristic about most faulty programs, that is, program inputs that can reveal failures (namely *failure-causing inputs*) tend to cluster together. Ammann and Knight (1988), for example, examined *failure regions* (that is, regions where failure-causing inputs reside) in some missile launch decision programs and observed that "at the resolution used in scanning, these particular failure regions are locally continuous". Bishop (1993) studied some faulty programs which implemented a nuclear reactor trip function, and found that all detected failures occupied contiguous regions (referred to as "blob defects" by Bishop (1993)). He also provided a theoretical justification for the existence of these "blob defects".

Chen et al. (2004c) employed the above-mentioned common characteristic of failure-causing inputs to improve the failure-detection capability of RT. They found that the effectiveness of RT can be significantly enhanced by evenly spreading random test cases over the whole input domain. This approach was named as *Adaptive Random Testing* (ART). Based on their work, many ART algorithms have been proposed, such as *Fixed-Sized-Candidate-Set ART* (FSCS-ART) (Chen et al., 2004c), *Lattice-based ART* (LART) (Mayer, 2005), and *Restricted Random Testing* (RRT) (Chan et al., 2006). These algorithms have been experimentally evaluated and it was confirmed that ART can use fewer test cases to detect the first failure than RT when failure-causing inputs are clustered into contiguous failure regions. As a consequence of using fewer test cases for detecting failures, ART can save testing resources, and the saving will become more significant when test case execution or test output verification is expensive. Briefly speaking, ART improves the performance of RT while keeping the randomness in the test case selection process, so it is intuitively appealing to consider ART as an

alternative to RT, especially when it takes considerable resources to execute test cases or to verify test results.

Some researchers (Mayer and Schneckenburger, 2006; Chen et al., 2007c) have pointed out that although all ART algorithms are based on the same intuition of evenly spreading test cases, they distribute test cases in different ways, and hence have different failure detection capabilities. For example, FSCS-ART and RRT prefer to select test cases from the edge part of the input domain rather than from the centre part. Due to such an *edge preference*, FSCS-ART and RRT may exhibit a certain degree of uneven test case distribution, and thus have a poor failure-detection capability under some situations (Chen et al., 2007c). Since we do not know where the failure-causing inputs are prior to testing, in order not to miss any failure-causing input, RT has normally been conducted based on the uniform distribution, that is, all inputs have equal chance to be selected as test cases. As an enhancement of RT, it is not desirable for ART to have any kind of preference of selecting test cases.

In this paper, we investigate how to offset the edge preference of two particular ART algorithms, namely FSCS-ART and RRT. We propose a new approach, which helps FSCS-ART and RRT distribute test cases more evenly, and hence improves their failure detection capabilities. The paper is organized as follows. Section 2 provides the preliminaries of FSCS-ART and RRT. Section 3 presents how we measure the edge preference of an ART algorithm. Section 4 explains how our approach offsets the edge preference. Some experiments have been conducted to evaluate the new approach. The experimental results are also reported in this section. Section 5 concludes the paper.

2 Preliminaries

2.1 Notation and Concepts

For ease of discussion, we introduce the following notation and concepts used in the rest of the paper.

- E denotes the set of all already executed test cases.
- $\mathcal{D}$ denotes the input domain. For the convenience of illustration, $\mathcal{D}$ is set to be a rectangle in the experiments of this paper. In this paper, $\mathcal{D}$ is assumed to be of numeric type (that is, input parameters accept either integers or real numbers). For applications of RT and ART on non-numeric programs, readers may consult the studies of Miller et al. (1990, 1995); Slutz (1998); Forrester and Miller (2000); Yoshikawa et al. (2003); Regehr (2005) and Merkel (2005); Kuo (2006); Ciupa et al. (2006, 2008), respectively.
- dD denotes d-dimension, where $d = 1, 2, 3, 4, \cdots$. The dimension of $\mathcal{D}$ refers to the number of input parameters of the program under test.
- $|E|$ and $|\mathcal{D}|$ denote the size of E and $\mathcal{D}$, respectively.
- Two basic features of all faulty programs.
    * *Failure rate*, denoted by θ, is defined as the ratio of the number of failure-causing inputs to the number of all possible inputs.
    * *Failure pattern* refers to the shapes of failure regions together with their distributions over $\mathcal{D}$.

  Both θ and failure pattern are fixed after coding but unknown before testing.

- *F-measure* refers to the expected number of test cases required to detect the first software failure. F-measure is more appropriate than other testing effectiveness metrics to measure ART/RT, as justified by Chen and Merkel (2008), so we will follow previous studies (Chen et al., 2004b,c, 2007c,d; Mayer, 2005; Chan et al., 2006) to use F-measure for evaluating the failure-detection capability of ART.
    * F_{RT} denotes the F-measure of RT. Theoretically, $F_{RT} = 1/\theta$ when test cases are selected with replacement, and according to uniform distribution.
    * F_{ART} denotes the F-measure of ART. As it has been reported by Chen et al. (2007d) that F_{ART} depends on many factors (such as θ, the dimension of $\mathcal{D}$, the compactness and the number of failure regions, the existence and the size of a predominant failure region), theoretical study of F_{ART} is extremely difficult. Hence, previous studies (Chen et al., 2004b,c, 2007c,d; Mayer, 2005; Chan et al., 2006) investigated F_{ART} through either simulations or empirical studies. For simulations, θ and the failure pattern were predefined. Test cases were selected using an ART algorithm. When a point is generated inside a failure region, a failure is said to be detected. The simulation was repeated for a sufficient number (S) of times to ensure that F_{ART} is accurate within a certain confidence level and a certain accuracy range (the details of calculating S can be found in the study of Chen et al. (2004b)). In this paper, the default values of confidence level and accuracy range are set as 95% and $\pm$5%, respectively.
    * *ART F-ratio* denotes $\dfrac{F_{ART}}{F_{RT}}$. ART F-ratio measures the improvement of ART over RT.

2.2 FSCS-ART

The *Fixed-Sized-Candidate-Set ART* (FSCS-ART) (Chen et al., 2004c) maintains two sets of test cases. One set is the *executed set* $E = \{e_1, e_2, \cdots, e_n\}$, as defined in the previous section; the other set is the *candidate set*, which contains k randomly generated inputs, denoted by $C = \{c_1, c_2, \cdots, c_k\}$, where k is fixed throughout the testing process. A candidate will be selected as the next test case if it has the longest distance to its nearest neighbour in E. Figure 1 shows the FSCS-ART algorithm. In this paper, the default value of k is set as 10, as recommended by Chen et al. (2004c).

1. Input an integer k, where $k > 1$.
2. Set $E = \{\}$ and $C = \{\}$.
3. Randomly generate a test case e from $\mathcal{D}$, according to uniform distribution.
4. Test the program with e as the test case.
5. **while** (e does not reveal a failure)
6. Add e into E.
7. Randomly generate k candidates from $\mathcal{D}$, according to uniform distribution, and construct $C = \{c_1, c_2, \cdots, c_k\}$.
8. **for** each candidate $c_j \in C$, where $j = 1, 2, \cdots, k$
9. Calculate the distance d_j between c_j and its nearest neighbour in E.
10. **end_for**
11. Find $c_b \in C$ such that $d_b \geq d_j$, $\forall j \in [1, k]$
12. Set $e = c_b$.
13. Test the program with e as the test case.
14. **end_while**
15. Report the detected failure and exit.

Figure 1: The algorithm of FSCS-ART

2.3 RRT

In *Restricted Random Testing* (RRT) (Chan et al., 2006), an *exclusion zone* is created around each element of E. The exclusion zone for each element of

E is of the same size $\frac{R \cdot |\mathcal{D}|}{|E|}$, where R is referred to as the *target exclusion ratio*. The RRT algorithm continuously generates inputs randomly from $\mathcal{D}$ until an input is generated outside all exclusion zones, which is then used as the next test case. Figure 2 shows details of the RRT algorithm.

1. Input an integer $maxTrial$ and a real number $initialR$, where $maxTrial > 0$ and $initialR > 0$.
2. Set $E = \{\}$.
3. Randomly generate a test case e from $\mathcal{D}$, according to uniform distribution.
4. Test the program with e as the test case.
5. **while** (e does not reveal a failure)
6. Add e into E.
7. Set $noTrial = 0$, $R = initialR$, and $outside =$ **false**.
8. **for** each element $e_i \in E$, where $i = 1, 2, \cdots, |E|$.
9. Determine a circular exclusion zone z_i, whose size is set as $\frac{R \cdot |\mathcal{D}|}{|E|}$.
10. **end_for**
11. **while** (**not** *outside*)
12. Increment $noTrial$ by 1.
13. **if** ($noTrial = maxTrial$)
14. Set $noTrial = 0$ and $R = R - 0.1$ (if $R < 0$, then set $R = 0$).
15. Redetermine all z_i.
16. **end_if**
17. Randomly generate a candidate c from $\mathcal{D}$, according to uniform distribution.
18. **if** ($c \notin \bigcup_{i=1}^{|E|} z_i$)
19. Set $outside =$ **true** and $e = c$.
20. **end_if**
21. **end_while**
22. Test the program with e as the test case.
23. **end_while**
24. Report the failure detected and exit.

Figure 2: The algorithm of RRT

Some simulations (Chan et al., 2006) have shown that the failure-detection capability of RRT becomes better with the increase of R, but a larger value of R means that a larger part of $\mathcal{D}$ would be excluded. Con-

sequently, a larger R may result in a longer computation time to find an appropriate test case. Previous studies have assumed a constant R. In this paper, two parameters ($initialR$ and $maxTrial$) were introduced to provide a facility that can dynamically reduce the value of R as a trade-off between the computation time and the even spreading of test cases. At first, R is set to be equal to $initialR$. If the RRT algorithm cannot find any appropriate input as the next test case after $maxTrial$ attempts, R will be reduced by a certain value (the reduction step value is set as 0.1 in this study). In this paper, we will use 1.0, 1.7, 3.3 and 6.4 as the default values of $initialR$ for 1D, 2D, 3D and 4D RRT, respectively, as recommended by Chan et al. (2006).

The algorithms in both Figures 1 and 2 are specifically used to evaluate the F-measure of ART. Therefore, the termination condition ("e does not reveal a failure" on Line 5 in Figures 1 and 2), is effectively set as "when the first failure is detected". It should be noted that when these ART algorithms are applied in real life, there are other possible termination conditions, such as "when a certain number of test cases have been selected", "when testing resources are exhausted", etc.

2.4 Edge preferences of FSCS-ART and RRT

Chen et al. (2007c) have pointed out that both FSCS-ART and RRT prefer to select test cases from the edge part of $\mathcal{D}$ rather than from the central part. Chen et al. (2007c) measured the edge preference of an ART algorithm by a metric, namely $M_{Edge:Centre}$, which is defined as the ratio of the number of test cases inside the subdomain $\mathcal{D}_{Edge}$ to the number of test cases inside the subdomain $\mathcal{D}_{Centre}$, where $\mathcal{D}_{Centre}$ is located in the centre of $\mathcal{D}$, $\mathcal{D}_{Edge}$ is right outside $\mathcal{D}_{Centre}$, and the sizes of $\mathcal{D}_{Centre}$ and $\mathcal{D}_{Edge}$ are equal. These two subdomains in a 2D space are illustrated in Figure 3. It was reported that

values of $M_{Edge:Centre}$ for FSCS-ART and RRT are always greater than 1, and the edge preference of RRT is more significant than that of FSCS-ART.

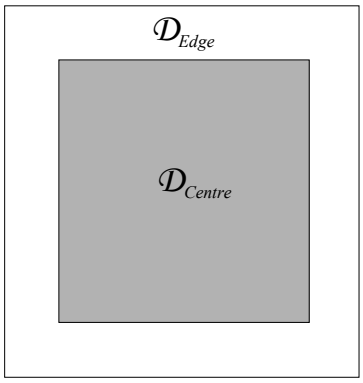

Figure 3: $\mathcal{D}_{Edge}$ and $\mathcal{D}_{Centre}$ in a 2D space

Some testing methods, such as the domain testing strategy (White and Cohen, 1980) and boundary-value analysis (Myers, 2004), select test cases close to or exactly on some "borders". However, the concept of "border" in these testing methods is different from the concept of "edge" in this study. For example, in the domain testing strategy, testers first divide $\mathcal{D}$ into regions based on the execution paths of the program under test. Test cases are then selected from near or on the borders of these regions. Obviously, these borders are not necessarily the boundary of $\mathcal{D}$. However, in FSCS-ART and RRT, the edge means the boundary of $\mathcal{D}$.

3 Measuring the Edge preference of an ART Algorithm

$M_{Edge:Centre}$ only coarsely measures the edge preference of an ART algorithm by two subdomains ($\mathcal{D}_{Centre}$ and $\mathcal{D}_{Edge}$). In this paper, we precisely describe

the edge preference of an ART algorithm by a graph, namely the frequency distribution graph of test cases with respect to the edge and the centre of $\mathcal{D}$ (abbreviated as $ECgraph$). The method of getting the $ECgraph$ of an ART algorithm is as follows.

(1) Partition $\mathcal{D}$ into m equal-sized and disjoint subdomains (denoted by $\mathcal{D}_i$, where $i = 1, 2, \cdots, m$) from the edge (where $i = 1$) to the centre (where $i = m$) of $\mathcal{D}$. Figure 6 illustrates the partitioning in a 2D space. In Figure 6, $\mathcal{D}$ is partitioned into $\mathcal{D}_1$, $\mathcal{D}_2$, $\mathcal{D}_3$ and $\mathcal{D}_4$, which are located from the edge to the centre of $\mathcal{D}$, respectively, and have the same size.

(2) Generate a set of test cases.

(3) Record the number of points in each subdomain.

(4) Calculate the normalized frequency of test cases in each subdomain.

(5) Repeat Steps (2)-(4) for a sufficient number of times to obtain reliable average values of frequencies with a confidence level of 95% and $\pm$5% accuracy range.

(6) Plot a curve in a 2D coordinate system, where the x-axis lists all subdomains from the edge ($\mathcal{D}_1$) to the centre ($\mathcal{D}_m$) of $\mathcal{D}$, and y-axis denotes the normalized frequency of test cases inside each subdomain.

Based on the average values of normalized frequencies in the $ECgraph$, two more statistical data can be collected, (i) the standard deviation of average normalized frequencies, denoted by M_{EC-SD}, and (ii) the difference between the maximal and minimal values of average normalized frequencies, denoted by M_{EC-MM}. Intuitively speaking, the smaller M_{EC-SD} and

M_{EC-MM} are, the more uniformly an ART algorithm distributes its test cases.

We conducted a series of simulations to obtain $ECgraphs$ of pure RT, FSCS-ART and RRT in 1D, 2D, 3D and 4D spaces. In these simulations, we set $m = 128$, because such a value ensures a sufficiently precise $ECgraph$ at an acceptable computation overhead. Furthermore, many previous studies (Merkel, 2005; Mayer and Schneckenburger, 2006; Chen et al., 2007a) have also used such a value for plotting the spatial distribution of test cases; and our setting will make it easier to compare different works in the future. $|E|$ was set as 10, 100, 1000, and 10000. The simulation results are shown in Figures 4 and 5. It has been observed that no matter what $|E|$ is, the normalized frequency for RT is always around 1/128 (that is, $1/m$), as theoretically expected, that is, the test cases of RT are always uniformly distributed. Therefore, in these figures, we only plot the $ECgraph$ of RT with $|E| = 10000$.

The values of M_{EC-SD} and M_{EC-MM} for RT, FSCS-ART, and RRT are summarized in Table 1.

Table 1: Values of M_{EC-SD} and M_{EC-MM} for RT, FSCS-ART, and RRT

dimension	*testing strategy*	|E| = 10		|E| = 100		|E| = 1000		|E| = 10000	
		$M_{EC\text{-}SD}$	$M_{EC\text{-}MM}$	$M_{EC\text{-}SD}$	$M_{EC\text{-}MM}$	$M_{EC\text{-}SD}$	$M_{EC\text{-}MM}$	$M_{EC\text{-}SD}$	$M_{EC\text{-}MM}$
1D	RT	8.56E-05	4.01E-04	2.95E-05	1.56E-04	1.78E-04	9.30E-04	6.09E-05	2.98E-04
	FSCS-ART	1.67E-03	1.16E-02	4.08E-04	5.10E-03	9.59E-05	6.55E-04	2.02E-05	9.75E-05
	RRT	1.44E-03	9.51E-03	3.85E-04	4.84E-03	8.63E-05	6.40E-04	2.28E-05	1.23E-04
2D	RT	9.00E-05	5.54E-04	2.67E-05	1.23E-04	2.10E-04	9.15E-04	6.11E-05	3.36E-04
	FSCS-ART	3.13E-03	1.13E-02	1.79E-03	9.70E-03	1.05E-03	9.05E-03	5.62E-04	6.77E-03
	RRT	3.47E-03	1.25E-02	2.62E-03	1.54E-02	1.62E-03	1.53E-02	8.94E-04	1.14E-02
3D	RT	9.33E-05	4.30E-04	2.99E-05	1.47E-04	2.08E-04	9.80E-04	5.87E-05	3.06E-04
	FSCS-ART	3.57E-03	1.12E-02	2.72E-03	1.00E-02	2.01E-03	9.44E-03	1.41E-03	9.23E-03
	RRT	4.52E-03	1.49E-02	4.95E-03	2.05E-02	3.88E-03	2.24E-02	2.74E-03	2.09E-02
4D	RT	9.36E-05	4.33E-04	2.80E-05	1.34E-04	2.08E-04	1.29E-03	5.51E-05	2.78E-04
	FSCS-ART	3.74E-03	1.23E-02	3.21E-03	1.05E-02	2.70E-03	1.01E-02	2.16E-03	9.69E-03
	RRT	5.02E-03	1.63E-02	6.28E-03	2.28E-02	5.53E-03	2.38E-02	4.37E-03	2.29E-02

Based on the experimental data, we make the following observations.

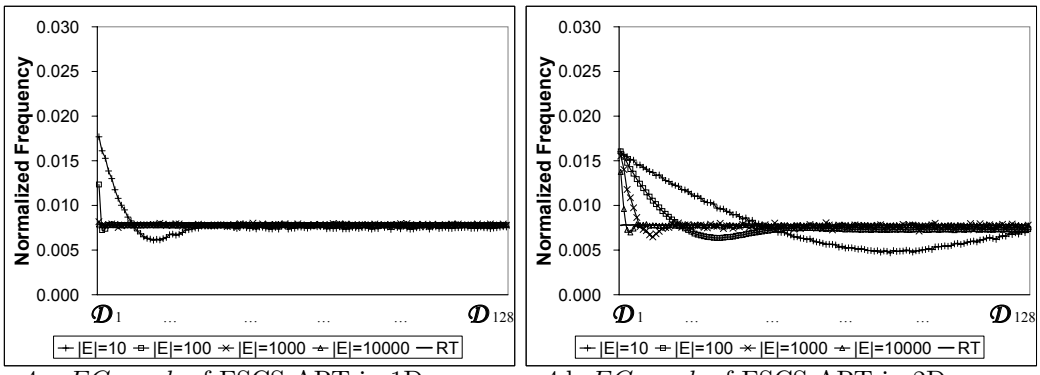

4.a *ECgraph* of FSCS-ART in 1D space

4.b *ECgraph* of FSCS-ART in 2D space

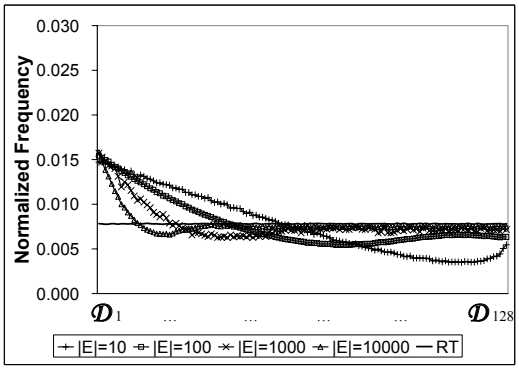

4.c *ECgraph* of FSCS-ART in 3D space

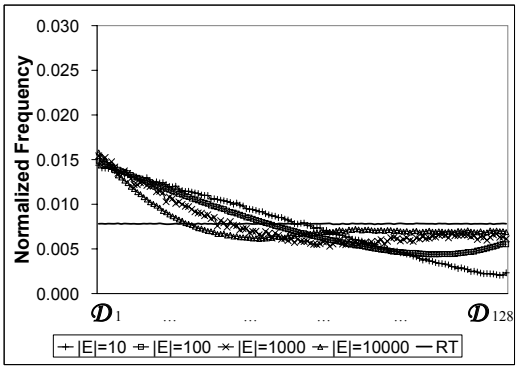

4.d *ECgraph* of FSCS-ART in 4D space

Figure 4: Frequency distribution of test cases selected by FSCS-ART with respect to the edge and the centre of input domain

(1) Both FSCS-ART and RRT have an edge preference.

(2) The edge preference becomes more significant with the increase of the dimension of $\mathcal{D}$.

(3) The edge preference becomes less significant with the increase of $|E|$.

(4) The edge preference of RRT is more significant than that of FSCS-ART for high dimension cases.

FSCS-ART and RRT algorithms evenly spread test cases by enforcing them far apart from one another; as a consequence, some of their test cases are pushed toward the edges of $\mathcal{D}$. In other words, the edge preference is

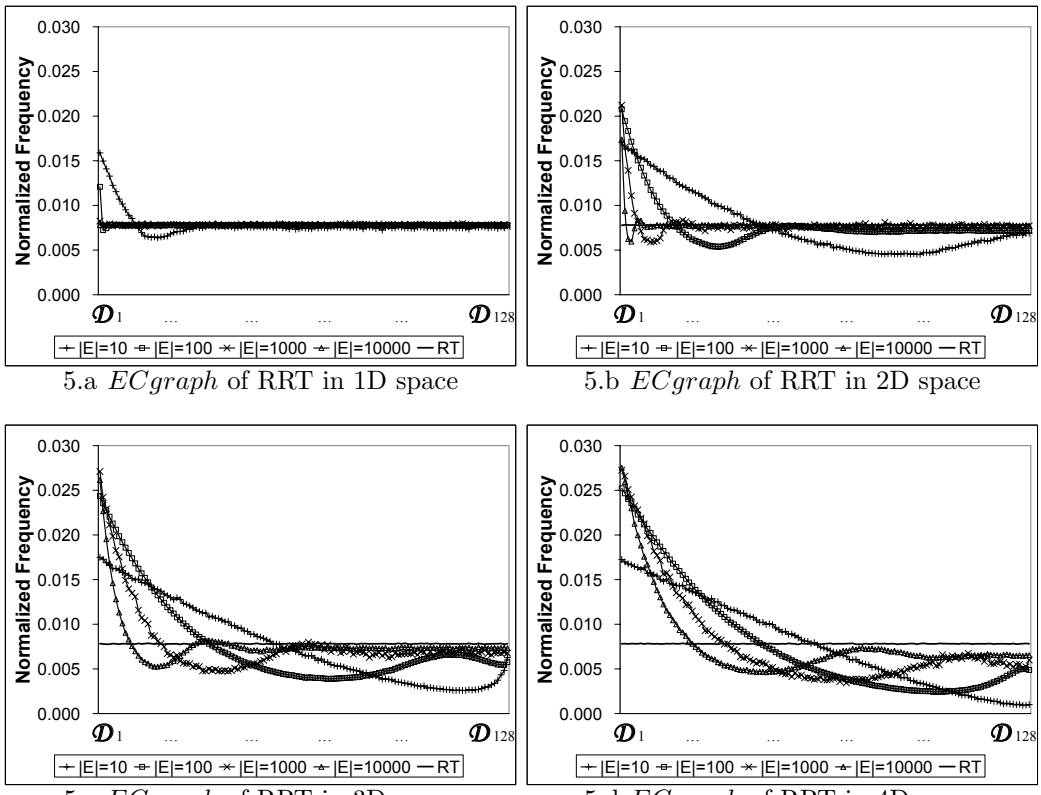

5.a *ECgraph* of RRT in 1D space

5.b *ECgraph* of RRT in 2D space

5.c *ECgraph* of RRT in 3D space

5.d *ECgraph* of RRT in 4D space

Figure 5: Frequency distribution of test cases selected by RRT with respect to the edge and the centre of input domain

a by-product of the test case selection procedures of FSCS-ART and RRT. However, it was observed that a poor failure-detection capability is always associated with a significant edge preference. As shown in the above experimental data, the edge preferences of FSCS-ART and RRT become more significant as $|E|$ decreases or the dimension of $\mathcal{D}$ increases. It was also reported that FSCS-ART and RRT have poorer failure detection capabilities for the cases of higher θ or higher dimension (Chen et al., 2007c). Such a correlation between the edge preference and the effectiveness of these ART algorithms has motivated us to improve these algorithms by offsetting their edge preferences.

4 Enhancing ART by offsetting the Edge preference

In this section, we will introduce a new approach to offsetting the edge preference of FSCS-ART and RRT algorithms. In this approach, $\mathcal{D}$ is partitioned into some equal-sized partitions from the edge to the centre of $\mathcal{D}$, and test cases will be evenly selected from these partitions. We integrate such a *Partitioning by Edge and Centre* (ECP) approach with the existing ART algorithms, and develop a new family of ART algorithms, namely ECP-ART algorithms. The new algorithms and their performances are elaborated in the following sections.

4.1 ART with partitioning by edge and centre

There are two instances of ECP-ART algorithms, ECP-FSCS-ART and ECP-RRT, which will be illustrated in a 2D space, as shown in Figures 6.a and 6.b, respectively. In these figures, $\mathcal{D}$ is partitioned into four equal-sized partitions $\mathcal{D}_1$, $\mathcal{D}_2$, $\mathcal{D}_3$ and $\mathcal{D}_4$, from the edge to the centre, respectively.

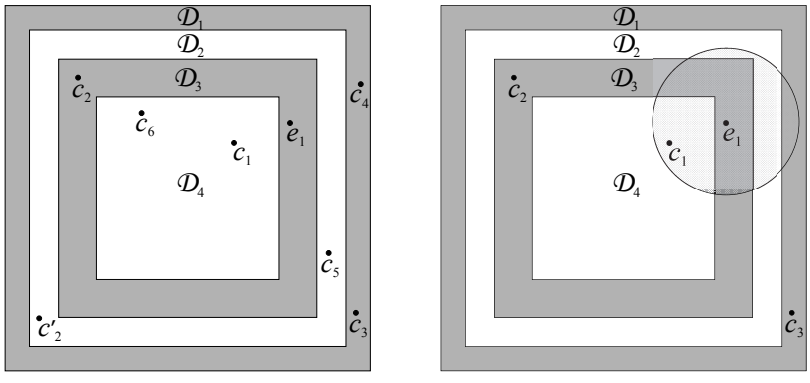

6.a ECP-FSCS-ART 6.b ECP-RRT

Figure 6: Illustration of ECP-ART algorithms

ECP-FSCS-ART is an integration of the ECP approach and FSCS-ART algorithm. Figure 6.a illustrates how it works. Suppose that the first test case e_1 is randomly generated from $\mathcal{D}$ and happens to be located inside $\mathcal{D}_3$. With regard to the selection of the next test case, six candidates, c_1, c_2, c_3, c_4, c_5 and c_6, are generated, as shown in Figure 6.a. However, since c_2 is inside the same partition as e_1, ECP-FSCS-ART requires a random replacement for c_2, say c_2' which is not located inside the same partition as e_1. Then, the second test case e_2 is selected from c_1, c_2' (instead of c_2), c_3, c_4, c_5 and c_6. Since c_2' is the farthest candidate from e_1, it will be selected as e_2.

For ECP-RRT (the integration of the ECP approach and RRT algorithm), refer to Figure 6.b. Suppose that the first random test case e_1 resides inside $\mathcal{D}_3$. A random input c_1 is generated and found to be inside the exclusion zone of e_1 (the shadowed circular zone around e_1). c_1 will be discarded, and then another input c_2 will be randomly generated, which happens to be outside the exclusion zone of e_1. Unfortunately, c_2 is in the same partition as e_1 (that is, $\mathcal{D}_3$). ECP-RRT will discard c_2, and then c_3 will be generated. c_3 will be selected as the next test e_2, because it is both outside the exclusion zone and the partition of e_1.

4.1.1 Details of new algorithms

There are two methods to implement the ECP approach. One method is to dynamically partition $\mathcal{D}$, that is, the number of partitions is varying with the number of executed test cases. The other method is static partitioning, that is, the number of partitions is fixed throughout the testing process. As reported by Chen et al. (2007b), the dynamic partitioning method performs better than the static method. Therefore, in this paper, we will focus on the ECP-ART algorithms with dynamic partitioning method. The details

of ECP-FSCS-ART and ECP-RRT algorithms are given in Figures 7 and 8, respectively.

1. Input an integer k, where $k > 1$.
2. Set $E = \{\}$ and $C = \{\}$.
3. Randomly generate a test case e from $\mathcal{D}$, according to uniform distribution.
4. Test the program with e as the test case.
5. **while** (e does not reveal a failure)
6. Add e into E.
7. Divide $\mathcal{D}$ into $|E| + 1$ disjoint partitions $\mathcal{D}_i$, from the edge to the centre of $\mathcal{D}$, where all $\mathcal{D}_i$ have the same size, and $i = 1, 2, \cdots, |E| + 1$.
8. Randomly generate k candidates from partitions where there does not exist any test case, and construct $C = \{c_1, c_2, \cdots, c_k\}$.
9. **for** each candidate $c_j \in C$, where $j = 1, 2, \cdots, k$
10. Calculate the distance d_j between c_j and its nearest neighbour in E.
11. **end_for**
12. Find $c_b \in C$ such that $d_b \geq d_j$, $\forall j \in [1, k]$
13. Set $e = c_b$.
14. Test the program with e as the test case.
15. **end_while**
16. Report the detected failure and exit.

Figure 7: The algorithm of ECP-FSCS-ART

As shown in Figures 7 and 8, ECP-ART always has $|E| + 1$ partitions. Therefore, at least one partition will not contain any executed test case. Our approach is to select the next test case from a "blank" partition. This will prevent test cases from being selected more frequently in certain subdomains, and hence offset the edge preference.

4.1.2 Runtime of new algorithms

Since the new algorithms are the integration of the ECP approach and the original ART algorithms, we will only analyze the computational overhead of the ECP approach. For each test case (except the first one) to be selected,

1. Input an integer $maxTrial$ and a real number $initialR$, where $maxTrial > 0$ and $initialR > 0$.
2. Set $E = \{\}$.
3. Randomly generate a test case e from $\mathcal{D}$, according to uniform distribution.
4. Test the program with e as the test case.
5. **while** (e does not reveal a failure)
6. Add e into E.
7. Divide $\mathcal{D}$ into $|E| + 1$ disjoint partitions $\mathcal{D}_i$, from the edge to the centre of $\mathcal{D}$, where all $\mathcal{D}_i$ have the same size, and $i = 1, \cdots, |E| + 1$.
8. Set $noTrial = 0$, $R = initialR$, and $outside =$ **false**.
9. **for** each element $e_i \in E$, where $i = 1, 2, \cdots, |E|$.
10. Determine a circular exclusion zone z_i, whose size is set as $\frac{R \cdot |\mathcal{D}|}{|E|}$.
11. **end_for**
12. **while** (**not** $outside$)
13. Increment $noTrial$ by 1.
14. **if** ($noTrial = maxTrial$)
15. Set $noTrial = 0$ and $R = R - 0.1$ (if $R < 0$, then set $R = 0$).
16. Redetermine all z_i.
17. **end_if**
18. Randomly generate a candidate c from partitions where there does not exist any executed test case.
19. **if** ($c \notin \bigcup_{i=1}^{|E|} z_i$)
20. Set $outside =$ **true** and $e = c$.
21. **end_if**
22. **end_while**
23. Test the program with e as the test case.
24. **end_while**
25. Report the failure detected and exit.

Figure 8: The algorithm of ECP-RRT

the ECP approach will first partition $\mathcal{D}$ into $|E|+1$ partitions; then identify the blank partitions, that is, the partitions which do not contain any executed test case; and finally, generate candidates from the blank partitions. Since $\mathcal{D}$ is of numeric type, it is very easy to calculate the value ranges for all partitions. For each executed test case, its corresponding partition can be identified simply through checking which value range each of its coordinates belongs to. Therefore, the identification of blank partitions requires $O(|E|)$ time. With regard to the candidate generation, it is basically the same as the random generation of any possible program input, except that the candidate must be selected within the value range of a blank partition $\mathcal{D}_i$ instead of from $\mathcal{D}$. Briefly speaking, it takes $O(|E|)$ time to implement the ECP approach in the process of selecting the $(|E|+1)$th test case, and thus the total computation overhead of the ECP approach for selecting $|E|$ test cases is in $O(|E|^2)$. Since FSCS-ART and RRT algorithms require $O(|E|^2)$ and $O(|E|^2 \log |E|)$ time to select $|E|$ test cases, respectively (Mayer and Schneckenburger, 2006), the orders of computation of ECP-ART and the original ART algorithms are the same.

We also experimentally evaluated the runtime of ECP-ART via some simulations. All simulations were conducted on a machine with an Intel Pentium processor running at 3195 MHz and 1024 megabytes of RAM. The ART algorithms were implemented in C language and compiled with GNU Compiler Collection (version 3.3.4) (GCC, 2004). FSCS-ART, ECP-FSCS-ART, RRT, and ECP-RRT were implemented in a 2D space. For each algorithm, we recorded the time taken to select a number of test cases, with $|E| = 500, 1000, 1500, 2000, 2500$, and 3000. The simulation results are given in Figure 9, in which, x- and y-axes denote $|E|$ and time required to generate E, respectively. It is clearly shown that FSCS-ART and ECP-FSCS-ART

both require $O(|E|^2)$ time to select $|E|$ test cases, while the runtimes of RRT and ECP-RRT are both in $O(|E|^2 \log |E|)$. In other words, the experimental data are consistent with the theoretical analysis.

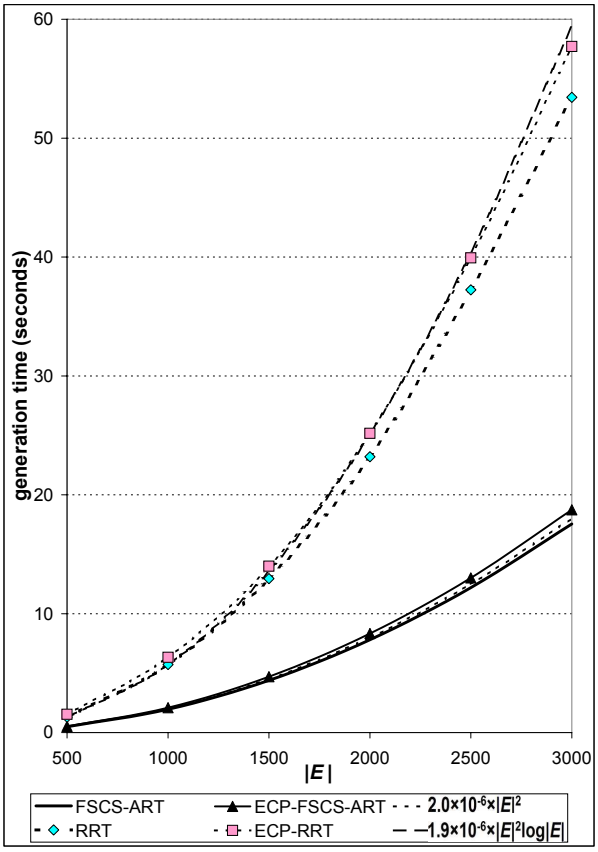

Figure 9: Comparison of runtime between the original ART algorithms and the new ECP-ART algorithms

4.2 Experiment 1

The intuition of ART is to enforce random test cases as evenly spread as possible. Thus, it is important to know how evenly ECP-ART algorithms spread their test cases. Chen et al. (2007c) have used three metrics to measure how test cases are evenly spread by various ART algorithms. Among

these metrics, $M_{Edge:Centre}$ has been discussed in Section 2.4. The other two metrics are discrepancy and dispersion, which are commonly used in measuring the equidistribution of sample points (Branicky et al., 2001). Intuitively speaking, discrepancy indicates whether regions have an equal density of the points; while dispersion indicates whether any point in E is surrounded by a very large empty spherical region (containing no points other than itself). E is considered reasonably equidistributed if discrepancy is close to 0, dispersion is small, and $M_{Edge:Centre}$ is close to 1 (that is, the edge preference is insignificant).

We first examine to what extent ECP-ART algorithms offset the edge preference. We repeated the simulations in Section 3 using ECP-FSCS-ART and ECP-RRT. The simulations results are shown in Figures 10 and 11, respectively. The values of M_{EC-SD} and M_{EC-MM} for ECP-FSCS-ART and ECP-RRT are summarized in Table 2.

Table 2: Values of M_{EC-SD} and M_{EC-MM} for ECP-FSCS-ART and ECP-RRT

dimension	*testing strategy*	|E| = 10		|E| = 100		|E| = 1000		|E| = 10000	
		$M_{EC\text{-}SD}$	$M_{EC\text{-}MM}$	$M_{EC\text{-}SD}$	$M_{EC\text{-}MM}$	$M_{EC\text{-}SD}$	$M_{EC\text{-}MM}$	$M_{EC\text{-}SD}$	$M_{EC\text{-}MM}$
1D	ECP-FSCS-ART	1.35E-03	9.65E-03	1.06E-04	7.77E-04	6.86E-05	3.15E-04	2.07E-05	1.22E-04
	ECP-RRT	1.02E-03	1.07E-02	1.76E-04	8.03E-03	7.85E-05	8.01E-03	2.11E-05	7.85E-03
2D	ECP-FSCS-ART	8.54E-04	3.13E-03	3.83E-04	2.22E-03	2.83E-04	2.22E-03	8.74E-05	7.64E-04
	ECP-RRT	9.97E-04	9.94E-03	8.14E-04	1.06E-02	4.98E-04	1.07E-02	2.88E-04	1.06E-02
3D	ECP-FSCS-ART	1.37E-03	4.07E-03	6.68E-04	2.58E-03	4.26E-04	2.38E-03	2.65E-04	2.08E-03
	ECP-RRT	1.28E-03	1.01E-02	1.66E-03	1.12E-02	1.23E-03	1.16E-02	8.49E-04	1.17E-02
4D	ECP-FSCS-ART	1.68E-03	4.80E-03	9.42E-04	2.98E-03	6.16E-04	2.84E-03	4.18E-04	2.30E-03
	ECP-RRT	1.86E-03	1.01E-02	2.23E-03	1.14E-02	1.82E-03	1.17E-02	1.38E-03	1.17E-02

Based on these data, we make the following three observations.

(1) ECP-ART algorithms distribute test cases more evenly than the original ART algorithms. Moreover, by comparing Figures 4 and 10 as well as Figures 5 and 11, it can be further observed that ECP-ART algorithms offset more edge preference for the cases where FSCS-ART and

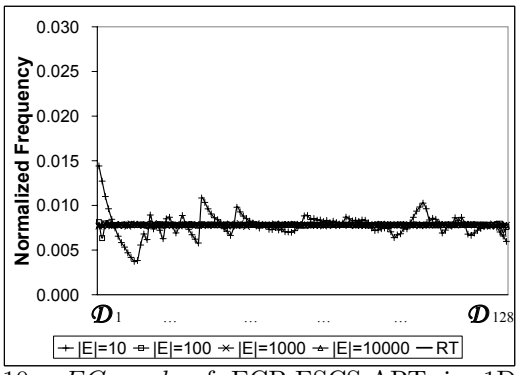

10.a *ECgraph* of ECP-FSCS-ART in 1D space

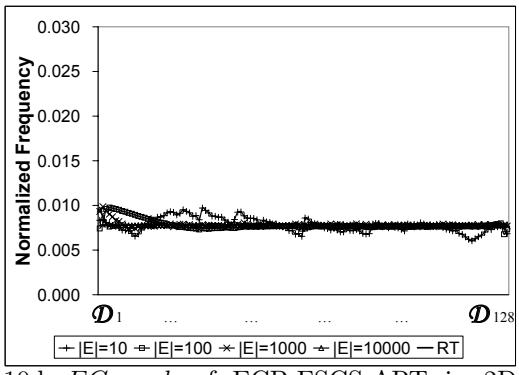

10.b *ECgraph* of ECP-FSCS-ART in 2D space

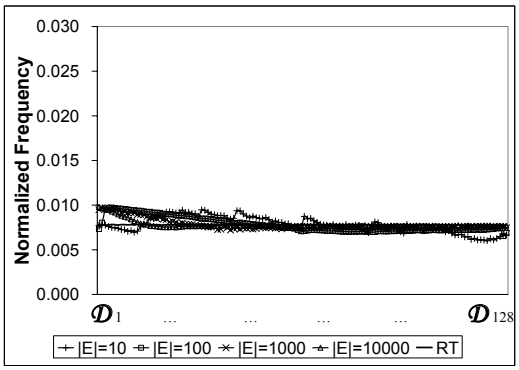

10.c *ECgraph* of ECP-FSCS-ART in 3D space

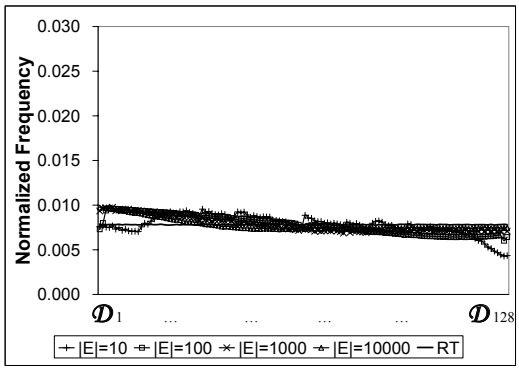

10.d *ECgraph* of ECP-FSCS-ART in 4D space

Figure 10: Frequency distribution of test cases selected by ECP-FSCS-ART with respect to the edge and the centre of input domain

RRT have a higher edge preference.

(2) There is still a small edge preference for ECP-ART algorithms.

(3) Based on Table 2, it can be observed that when the dimension of $\mathcal{D}$ is higher than 1, ECP-FSCS-ART algorithm has a smaller edge preference than ECP-RRT algorithm.

The first observation is consistent with the intuition of our study, that is, the edge preference can be offset by ECP-ART algorithms. It has been observed in Section 3 that the higher dimension of $\mathcal{D}$ or the higher θ, the

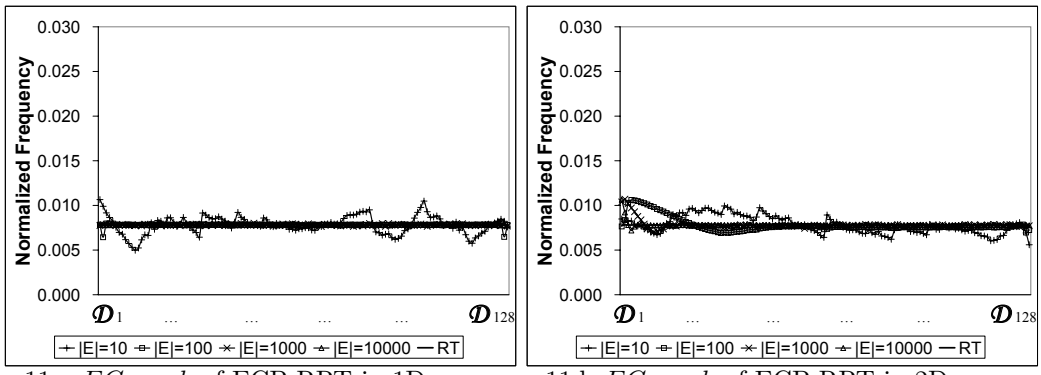

11.a *ECgraph* of ECP-RRT in 1D space

11.b *ECgraph* of ECP-RRT in 2D space

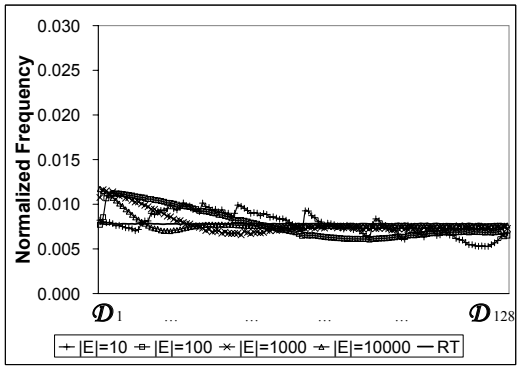

11.c *ECgraph* of ECP-RRT in 3D space

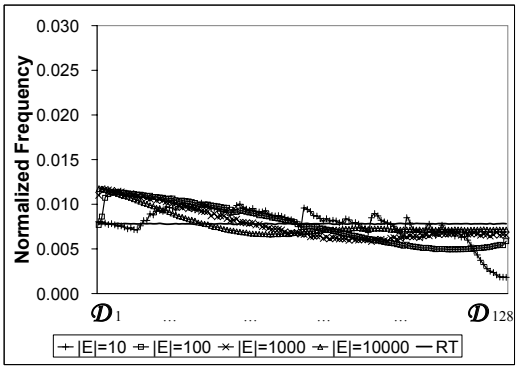

11.d *ECgraph* of ECP-RRT in 4D space

Figure 11: Frequency distribution of test cases selected by ECP-RRT with respect to the edge and the centre of input domain

more significant edge preference of FSCS-ART and RRT. Therefore, it is expected that ECP-ART algorithms have a more noticeable offset of the edge preference when the dimension is higher or θ is higher. The second observation can be explained as follows. Although the next test case is from a "blank" partition, there can be more than one blank partition. Due to the nature of FSCS-ART and RRT, inputs from the blank partition near $\mathcal{D}$'s edge have a higher probability to be selected as the next test case than inputs from the blank partition near $\mathcal{D}$'s centre. The last observation is also understandable. Since the edge preference of the original RRT algorithm is more significant than that of the original FSCS-ART algorithm when the

dimension of $\mathcal{D}$ is high, it is intuitive for ECP-RRT to have a more significant edge preference than ECP-FSCS-ART for higher dimensions.

In order to further investigate the test case distributions of ECP-ART algorithms, we repeated the simulations in the study of Chen et al. (2007c) on ECP-FSCS-ART and ECP-RRT, and got their discrepancies and dispersions. Since we found that ECP-RRT distributes test cases similarly as ECP-FSCS-ART, we only report the values of discrepancy and dispersion for ECP-FSCS-ART, as shown in Figures 12 and 13, respectively. For ease of comparison, the previous simulation results of FSCS-ART are also included in these figures. These figures clearly show that ECP-FSCS-ART has a smaller $M_{Discrepancy}$ than FSCS-ART, and its $M_{Dispersion}$ is similar to that of FSCS-ART.

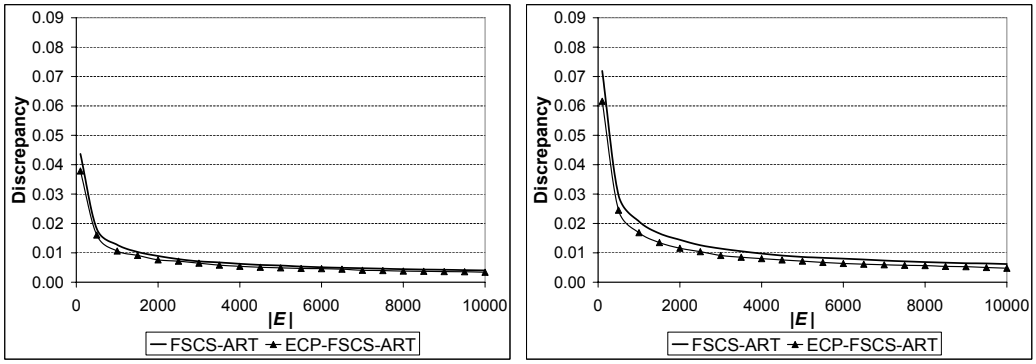

12.a discrepancy in 1D space

12.b discrepancy in 2D space

12.c discrepancy in 3D space

12.d discrepancy in 4D space

Figure 12: Comparison of discrepancy between ECP-FSCS-ART and FSCS-ART

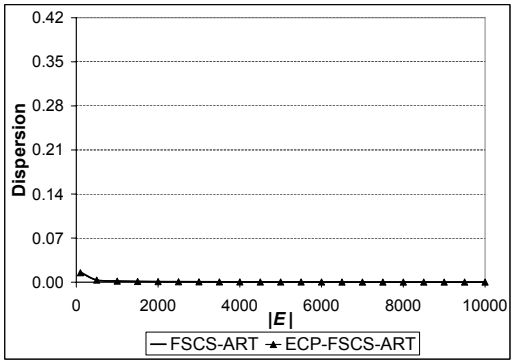

13.a dispersion in 1D space

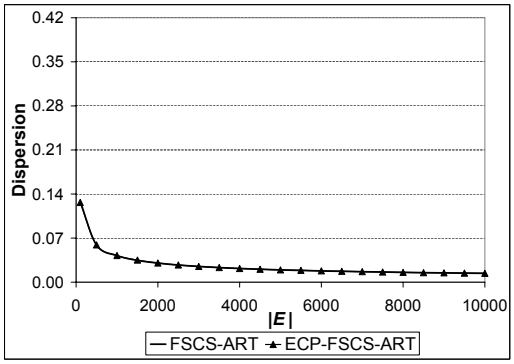

13.b dispersion in 2D space

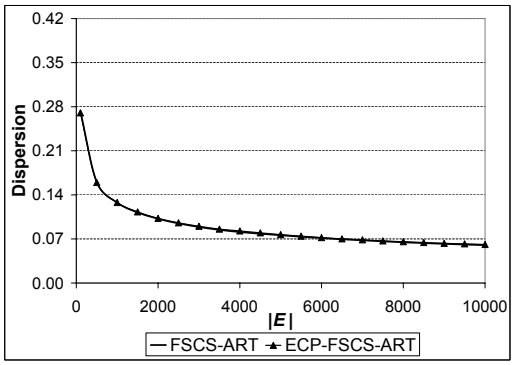

13.c dispersion in 3D space

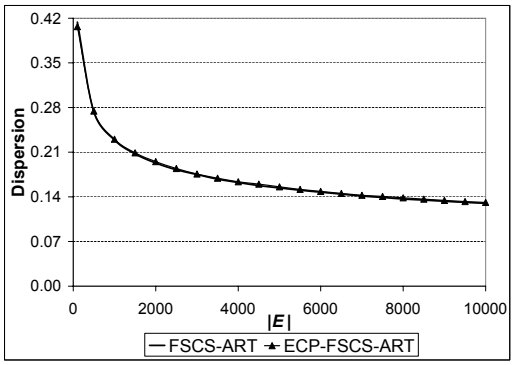

13.d dispersion in 4D space

Figure 13: Comparison of dispersion between ECP-FSCS-ART and FSCS-ART

In summary, ECP-ART algorithms can offset the edge preference very well, and spread test cases more evenly than the original ART algorithms.

4.3 Experiment 2

The previous section concludes that the new ECP-ART algorithms distribute test cases more evenly than original ART algorithms. We are now going to examine whether the failure detection capabilities can be improved, through a series of simulations. The parameters for these simulations are set as follows.

- Dimension of $\mathcal{D}$: 1, 2, 3 and 4.

- θ: 0.75, 0.5, 0.25, 0.1, 0.075, 0.05, 0.025, 0.01, 0.0075, 0.005, 0.0025, 0.001, 0.00075, 0.0005, 0.00025, 0.0001, 0.000075, and 0.00005.
- Failure pattern: a single square failure region is randomly placed inside $\mathcal{D}$.

It should be noted that the setting of this experiment is exactly the same as Experiment 1 in the study of Chen et al. (2007d). The results of these simulations are reported in Figure 14, which also includes the previous simulation results of FSCS-ART and RRT for ease of comparison. Note that the scales in Figure 14 do not start at 0.

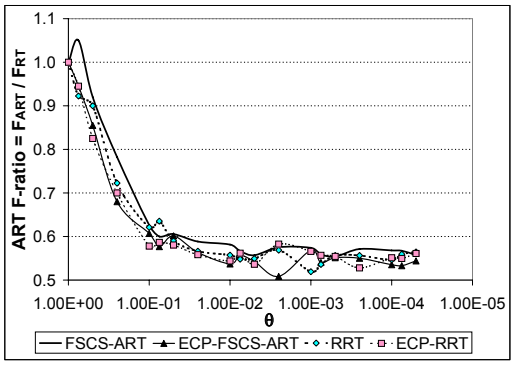

14.a Comparison in 1D space

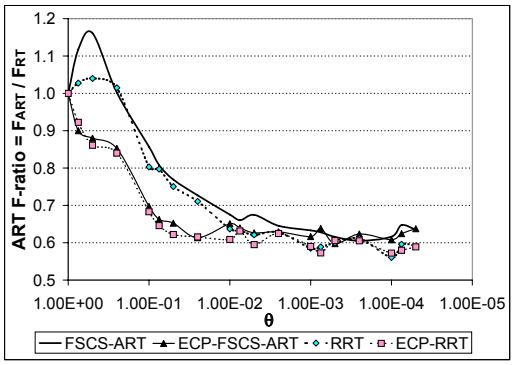

14.b Comparison in 2D space

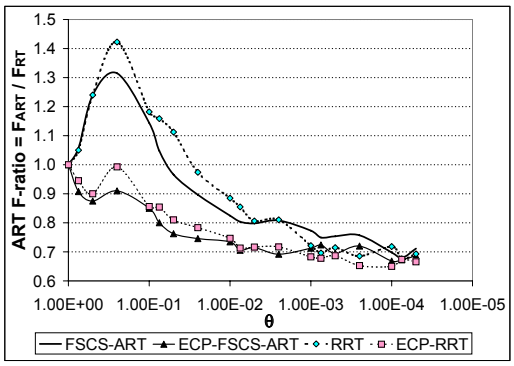

14.c Comparison in 3D space

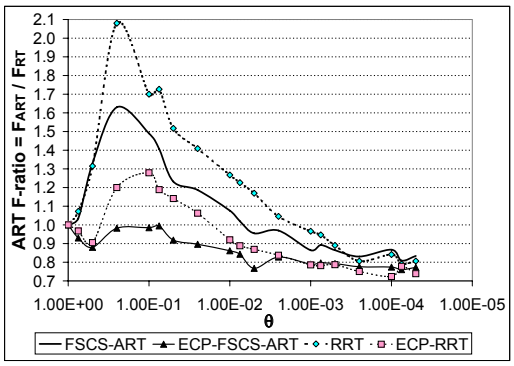

14.d Comparison in 4D space

Figure 14: Comparison of failure detection capabilities between the original ART algorithms and the new ECP-ART algorithms

We have reached the following conclusions.

(1) When the dimension of $\mathcal{D}$ or θ is high, the failure detection capabilities of ECP-ART algorithms are better than those of the original ART algorithms; otherwise, the performances of ECP-ART and the original ART algorithms are more or less similar.

(2) ECP-FSCS-ART is more effective than ECP-RRT for the cases of high dimension and high θ.

The first conclusion is expected. As explained in Section 4.2, the higher the dimension of $\mathcal{D}$ or θ is, the more edge preference will be offset by ECP-ART algorithms. Since ECP-ART algorithms are introduced to enhance the failure detection capabilities of the original ART algorithms by offsetting their edge preferences, it is expected that the higher the dimension of $\mathcal{D}$ or θ, the better improvement of the failure-detection capability of ECP-ART over the original ART algorithms. It is also understandable to have the second conclusion that ECP-FSCS-ART has better failure-detection capability than ECP-RRT for higher θ cases, because the former can distribute test cases more evenly than the latter (the last observation in Section 4.2).

As a summary of experiments reported in Sections 4.2 and 4.3, the new partitioning approach enhances the original ART algorithms not only in terms of the even distribution of test cases, but also with respect to the failure-detection capability. As shown in these experiments, ECP-FSCS-ART and ECP-RRT algorithms have similar performance trends, so we will only investigate ECP-FSCS-ART in the rest of the experimental study.

4.4 Experiment 3

Chen et al. (2007d) have pointed out that besides θ and the dimension of $\mathcal{D}$, the failure-detection capability of FSCS-ART also depends on (a) how

compact the failure region is, (b) how many failure regions there are, (c) whether there exists a predominant failure region by size, and (d) how large the predominant failure region is. In this section, we conducted a similar investigation for ECP-FSCS-ART.

We first conducted a simulation to see how the compactness of a failure region influences the failure-detection capability of ECP-FSCS-ART. The simulation used the rectangle (instead of the square in Section 4.3) as the shape of the failure region in order to investigate the impact of compactness. The experimental setting is as follows.

- Dimension of $\mathcal{D}$: 2, 3 and 4.
- θ: 0.005.
- Failure pattern: a single rectangular region is randomly placed inside the input domain. The ratios among edge lengths of the rectangular region are $1 : \alpha$, $1 : \alpha : \alpha$ and $1 : \alpha : \alpha : \alpha$ in 2D, 3D and 4D spaces, respectively, where $\alpha \geq 1$.
- α: 1, 4, 7, 10, 20, 30, 40, 50, 60, 70, 80, 90 and 100. As justified by Chen et al. (2007d), the larger α is, the less compact the failure region is.

The above experimental setting is similar to the setting of Experiment 2 in the study of Chen et al. (2007d). The simulation results are reported in Figure 15, which also includes the previous simulation results on FSCS-ART for ease of comparison. As shown in Figure 15, although the effectiveness of ECP-FSCS-ART also depends on the compactness of a failure region, ECP-FSCS-ART outperforms FSCS-ART in most scenarios, and the performance improvement is more significant with the increase of dimension.

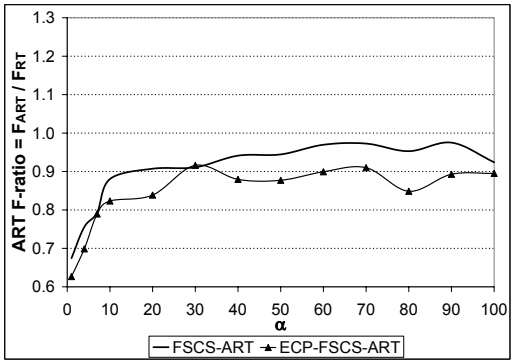

15.a 2D, $\theta = 0.005$

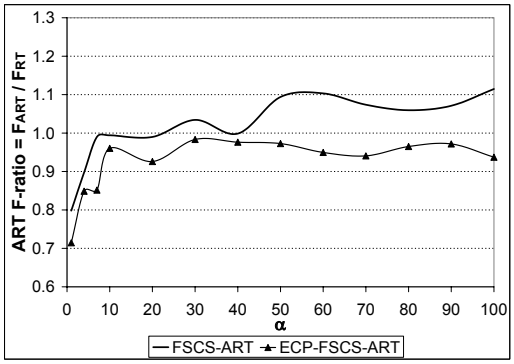

15.b 3D, $\theta = 0.005$

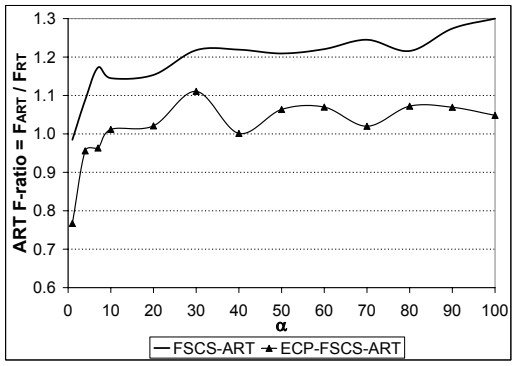

15.c 4D, $\theta = 0.005$

Figure 15: Failure detection capabilities of ECP-FSCS-ART on a rectangular failure region

We conducted another simulation to evaluate the failure-detection capability of ECP-FSCS-ART where there are more than one failure region. The experimental setting of this simulation is as follows.

- Dimension of $\mathcal{D}$: 2, 3 and 4.
- θ: 0.005.
- Failure pattern: a number of equal-sized square regions are randomly placed inside the input domain.
- The number of failure regions: 1, 4, 7, 10, 20, 30, 40, 50, 60, 70, 80, 90 and 100.

It should be noted that the above setting is similar to the experimental setting of Experiment 3 in the study of Chen et al. (2007d). Figure 16 shows the simulation results. It can be observed that ECP-FSCS-ART behaves similarly as FSCS-ART, that is, its effectiveness depends on the number of failure regions. But ECP-FSCS-ART has a better failure-detection capability, especially when the dimension of $\mathcal{D}$ is higher.

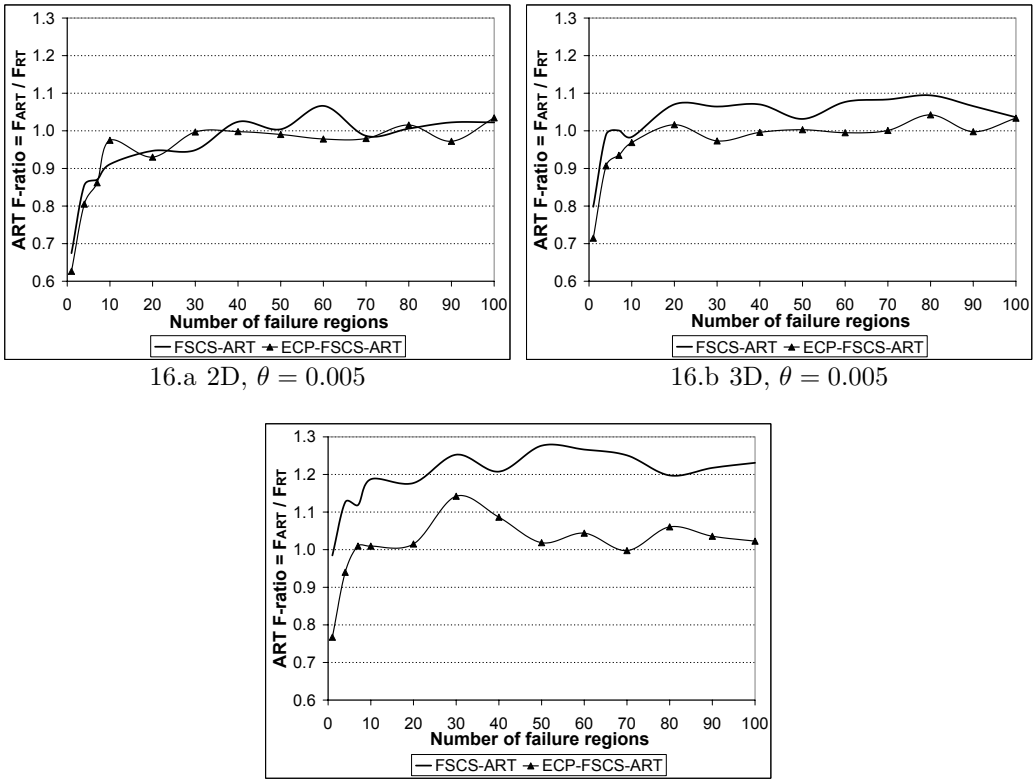

16.a 2D, $\theta = 0.005$

16.b 3D, $\theta = 0.005$

16.c 4D, $\theta = 0.005$

Figure 16: Failure detection capabilities of ECP-FSCS-ART on multiple equal-sized failure regions

In the above simulation, all the failure regions have the same size. However, it is unlikely that all failure regions are equal-sized in reality. Therefore, we further conducted a simulation where failure regions are of different sizes. This simulation has the following experimental setting.

- Dimension of $\mathcal{D}$: 2, 3 and 4.
- θ: 0.005.
- Failure pattern: a number of square regions are randomly placed inside the input domain. Suppose that there are n failure regions, denoted by $R_1, R_2, \cdots, R_n$, respectively. The sizes of these regions $(|R_1|, |R_2|, \cdots, |R_n|)$ are assigned by either of the following two ways.
  * Existence of a predominant failure region. For one region R_n, set $|R_n| = r \cdot \theta \cdot |\mathcal{D}|$, where $r = 0.3, 0.5$ and 0.8. For all the other regions, $|R_i| = \frac{v_i}{\sum_{i=1}^{n-1} v_i} \cdot (1 - r) \cdot \theta \cdot |\mathcal{D}|$, where v_i is a random number uniformly distributed in $[0, 1)$, and $i = 1, 2, \cdots, n - 1$.
  * No predominant failure region. For all regions, $|R_i| = \frac{v_i}{\sum_{i=1}^{n} v_i} \cdot \theta \cdot |\mathcal{D}|$, where v_i is a random number uniformly distributed in $[0, 1)$, and $i = 1, 2, \cdots, n$.
- The number of failure regions: 1, 4, 7, 10, 20, 30, 40, 50, 60, 70, 80, 90 and 100.

The above setting is similar to the setting of Experiment 4 in the study of Chen et al. (2007d). The simulation results of ECP-FSCS-ART as well as the previous results of FSCS-ART are given in Figure 17. We can observe that the performance of ECP-FSCS-ART also depends on the existence and the size of a predominant failure region, and ECP-FSCS-ART generally has a better failure-detection capability than the original FSCS-ART.

Based on experiments reported in Sections 4.3 and 4.4, we conclude that like FSCS-ART, the failure-detection capability of ECP-FSCS-ART also depends on θ, the dimension of $\mathcal{D}$, the compactness and the number of failure

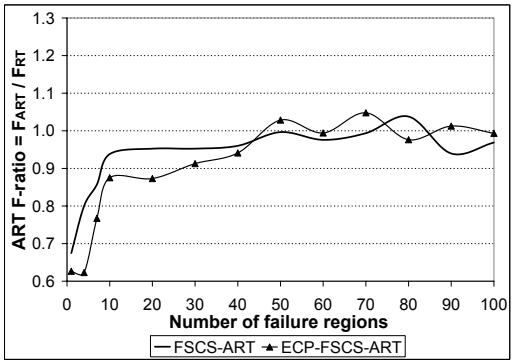

17.a No predominant failure region, 2D

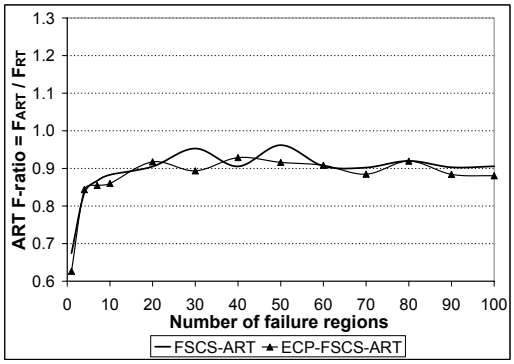

17.d Predominant failure region exists, 2D, $r = 0.3$

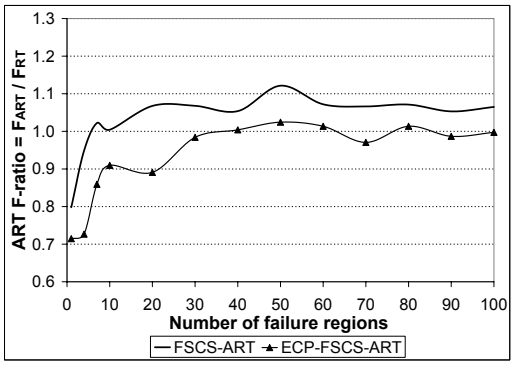

17.b No predominant failure region, 3D

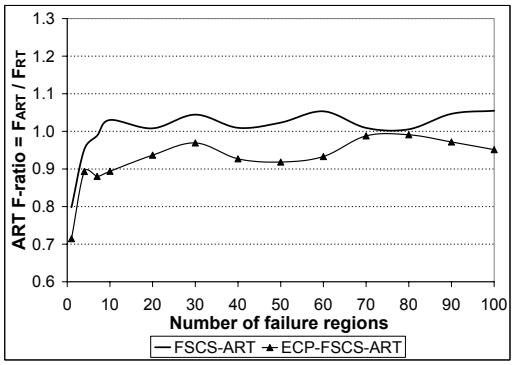

17.e Predominant failure region exists, 3D, $r = 0.3$

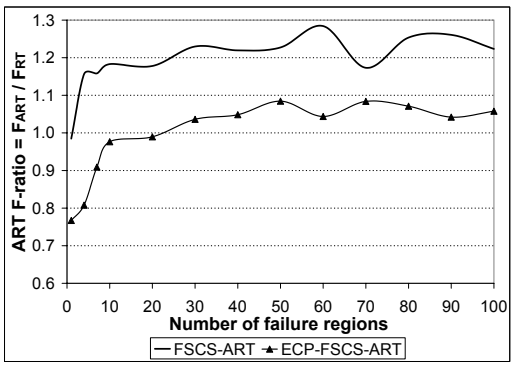

17.c No predominant failure region, 4D

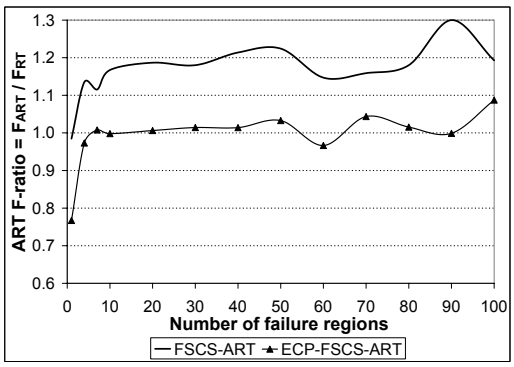

17.f Predominant failure region exists, 4D, $r = 0.3$

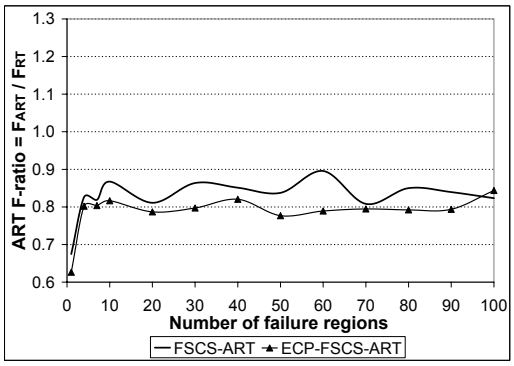

17.g Predominant failure region exists, 2D, $r = 0.5$

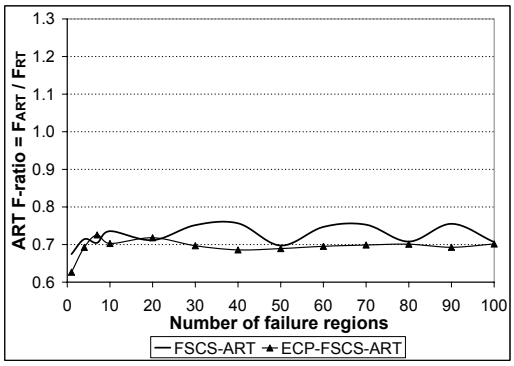

17.j Predominant failure region exists, 2D, $r = 0.8$

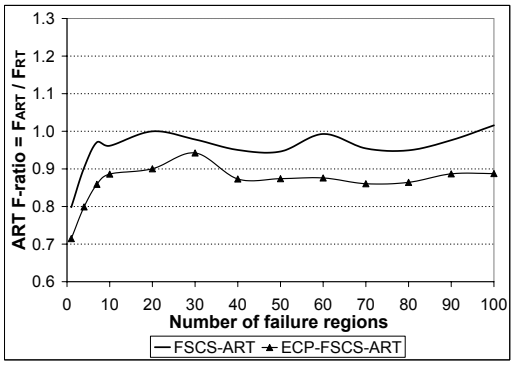

17.h Predominant failure region exists, 3D, $r = 0.5$

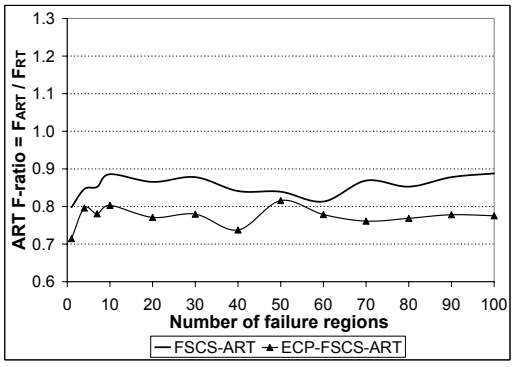

17.k Predominant failure region exists, 3D, $r = 0.8$

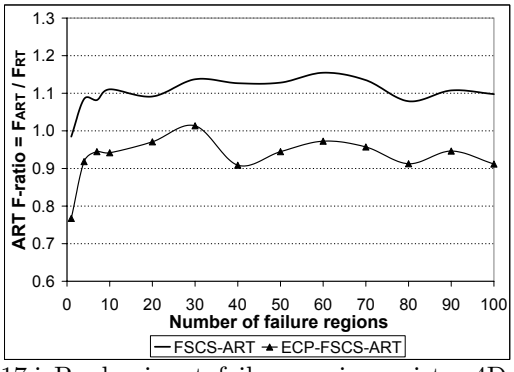

17.i Predominant failure region exists, 4D, $r = 0.5$

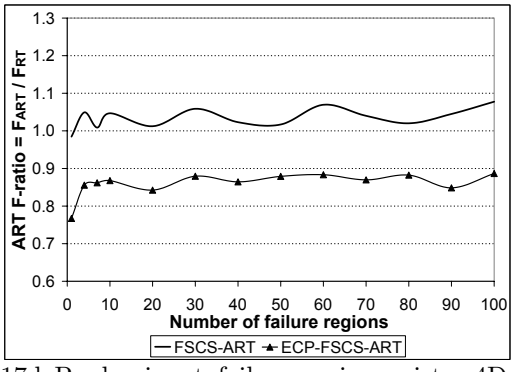

17.l Predominant failure region exists, 4D, $r = 0.8$

Figure 17: Failure detection capabilities of ECP-FSCS-ART on multiple failure regions with various sizes, where $\theta = 0.005$

regions, the existence and the size of a predominant failure region. But ECP-FSCS-ART generally outperforms the original FSCS-ART, and the performance improvement becomes more significant when the dimension of $\mathcal{D}$ or θ is higher.

4.5 Experiment 4

Chen et al. (2004c) have also applied the original FSCS-ART to test some real-life programs, which are all published programs (ACM, 1980; Press et al., 1986), and were error-seeded using the technique of mutation (Budd, 1981). As shown in Section 4.3, the failure-detection capability of ECP-FSCS-ART is dependent on the dimension of $\mathcal{D}$. Therefore, in this experimental study, we selected four particular programs as the subject programs with varying dimensions, namely *airy*, *bessj*, *plgndr*, and *el2*, whose input domains are 1D, 2D, 3D, and 4D, respectively. The details of these 4 programs are given in Table 3.

Table 3: Program name, dimension, and seeded errors for each subject program

Program	Dimension	Number of seeded errors			
		AOR	ROR	SVR	CR
airy	1				1
bessj	2	2	1		1
plgndr	3	1	2		2
el2	4	1	3	2	3

AOR	arithmatic operator replacement
ROR	relational operator replacement
SVR	scalar variable replacement
CR	constant replacement

For each subject program, Chen et al. (2004c) defined its input domain by setting the value ranges for all of its input parameters. After defining

the input domains, they estimated the failure rates (θ) of these programs by finding the F-measures of RT and then applying the formula $\theta = 1/F_{RT}$. In this study, we aim to investigate the impact of the relative locations of failure regions on the ART performance. Hence, we kept the same seeded errors for these subject programs, but modified the relative locations of failure regions by changing the range values for the input domains. Refer to Table 4, where *airy*, *bessj*, *plgndr*, and *el2* denote the programs on original input domains (which were defined by Chen et al. (2004c)), while *airy_new*, *bessj_new*, *plgndr_new* and *el2_new* denote the programs on newly-defined input domains. The modification of the input domains only have strong impacts on the locations of failure regions and θ of subject programs; while the basic shapes of the failure regions remain unchanged because the seeded errors are not changed.

Table 4: The failure rates and failure patterns of subject programs on different input domains

Program	Input domain		Failure rate	Failure pattern
	From	To	(θ)	
airy	(-5000)	(5000)	0.000716	A block in the centre of input domain
airy_new	(0)	(10000)	0.000694	A block on the edge of input domain
bessj	(2, -1000)	(300, 15000)	0.001298	Strips near the edge of input domain
bessj_new	(-100, -8000)	(200, 8000)	0.001279	Strips in the centre of input domain
plgndr	(10, 0, 0)	(500, 11, 1)	0.000368	Strips near the edge of input domain
plgndr_new	(-300, -6, -1)	(300, 6, 1)	0.000965	Strips spanning from the centre to the edge of input domain
el2	(0, 0, 0, 0)	(250, 250, 250, 250)	0.000690	Strips near the edge of input domain
el2_new	(-200,-200,-200,-200)	(200, 200, 200, 200)	0.000703	Strips crossing the centre of input domain

We applied the original FSCS-ART algorithm to test *airy_new*, *bessj_new*, *plgndr_new* and *el2_new*. The experimental results are shown in Table 5, which also includes the previous results on *airy*, *bessj*, *plgndr*, and *el2*. It is clearly shown that as expected, for the same program, FSCS-ART has fairly different failure detection capabilities for different locations of failure regions.

Table 5: Failure detection capabilities of FSCS-ART on 4 programs with different input domains

Program	FSCS-ART F-ratio	
	original input domains	new input domains
airy	0.5786	0.3564
bessj	0.5817	0.8102
plgndr	0.6591	0.8462
el2	0.4798	1.0845

We repeated the experiment by applying ECP-FSCS-ART to test all four subject programs on both the original and the new input domains. The experimental results are shown in Table 6. As intuitively expected, ECP-FSCS-ART performs similarly on the same program under various scenarios.

Table 6: Failure detection capabilities of ECP-FSCS-ART on 4 programs with different input domains

Program	ECP-FSCS-ART F-ratio	
	original input domains	new input domains
airy	0.5338	0.5534
bessj	0.6347	0.6717
plgndr	0.7011	0.7456
el2	0.7744	0.8289

In summary, the failure-detection capability of ECP-FSCS-ART is less dependent on the locations of failure regions than that of FSCS-ART.

5 Discussion and Conclusion

ART was originally proposed as an approach to enhancing the failure-detection capability of RT. Recent studies have pointed out that some ART algorithms prefer to select test cases from the edge part of the input domain. Since we do not know where the failure-causing inputs are prior to testing, it

is not desirable for inputs to have different chances of being selected as test cases. In this paper, we investigated the edge preferences of FSCS-ART and RRT, and proposed a new family of algorithms, namely ART with Partitioning by Edge and Centre (ECP-ART).

ECP-ART uses an additional partitioning scheme to offset the edge preference. The new ECP-ART algorithms have the same orders of computation as the original ART algorithms. Compared with the original ART algorithms, ECP-ART algorithms have similar values of dispersion, but smaller values of discrepancy. In other words, ECP-ART can spread test cases more evenly than the original ART algorithms. It has also been observed that the effectiveness of ECP-ART depends on the same factors as the original ART algorithms. However, ECP-ART algorithms normally have better failure detection capabilities under the same conditions, and the performance enhancement of ECP-ART over the original ART algorithms becomes more significant with the increase of dimension or failure rate. It has also been shown by simulations and experimental studies that the failure detection capabilities of the new ECP-ART algorithms are less dependent on the locations of failure regions than those of the corresponding ART algorithms. In summary, the basic idea of our new approach is that for an ART algorithm which prefers to select test cases from certain locations of the input domain, we offset the preference by using a specifically designed partitioning scheme.

As a pilot study, this paper only investigated how to apply such an idea into FSCS-ART and RRT algorithms. Mayer and Schneckenburger (2006) have pointed out that most ART algorithms have a preference toward test cases from certain locations of the input domain. For example, *ART through Iterative Partitioning* (ART-IP) (Chen et al., 2006) has a similar test case distribution as FSCS-ART; while *Lattice-based ART* (LART) (Mayer, 2005)

exhibits a preference on some small square regions inside the input domain. Chen et al. (2007c) also observed that *ART by Random Partitioning* (ART-RP) (Chen et al., 2004a) has a small centre preference (that is, inputs from the centre part of the input domain has a high probability of being selected as test cases). Intuitively speaking, the basic idea of this paper can also be applied to these ART algorithms, as long as we can find appropriate partitioning schemes that can offset the preferences of these algorithms. The ECP approach proposed in this paper is applicable for ART-IP and ART-RP. For LART and many other ART algorithms (such as *Mirror ART* (Chen et al., 2004b) and *ART by Localization* (Chen and Huang, 2004)), since they have more complicated test case distributions than FSCS-ART and RRT, further investigations are required to find appropriate partitioning schemes for them.

There exists one particular ART algorithm, namely *ART by Bisection* (ART-B) (Chen et al., 2004a), which does not exhibit any preference in the test case selection. Chen et al. (2007c) have observed that FSCS-ART and RRT only outperform ART-B when the failure rate is small. We have compared the failure detection capabilities of ART-B and ECP-ART, and found that ECP-ART normally has a better failure-detection capability than ART-B, no matter whether the failure rate is high or not.

In conclusion, this paper has proposed a new approach that can help some ART algorithms spread test cases more evenly and detect software failures more effectively. The basic idea of the new approach is not only applicable and useful to FSCS-ART and RRT, but also to many other ART algorithms.

Acknowledgment

This research project is supported by an Australian Research Council Discovery Grant (DP0880295).

References

ACM, 1980. Collected Algorithms from ACM. Association for Computing Machinery.

Ammann, P. E., Knight, J. C., 1988. Data diversity: an approach to software fault tolerance. IEEE Transactions on Computers 37 (4), 418–425.

Bishop, P. G., 1993. The variation of software survival times for different operational input profiles. In: Proceedings of the 23rd International Symposium on Fault-Tolerant Computing (FTCS-23). IEEE Computer Society Press, pp. 98–107.

Branicky, M. S., LaValle, S. M., Olson, K., Yang, L., 2001. Quasi-randomized path planning. In: Proceedings of the 2001 IEEE International Conference on Robotics and Automation. IEEE Computer Society, pp. 1481–1487.

Budd, T. A., 1981. Mutation analysis: Ideas, examples, problems and prospects. In: Chandrasekaran, B., Radicci, S. (Eds.), Computer Program Testing. North-Holland, Amsterdam, pp. 129–148.

Chan, K. P., Chen, T. Y., Towey, D., 2006. Restricted random testing: Adaptive random testing by exclusion. International Journal of Software Engineering and Knowledge Engineering 16 (4), 553–584.

Chen, T. Y., Eddy, G., Merkel, R., Wong, P. K., 2004a. Adaptive random testing through dynamic partitioning. In: Proceedings of the 4th International Conference on Quality Software (QSIC 04). IEEE Computer Society Press, Braunschweig, Germany, pp. 79–86.

Chen, T. Y., Huang, D. H., 2004. Adaptive random testing by localization. In: Proceedings of the 11th Asia-Pacific Software Engineering Conference (APSEC'04). IEEE Computer Society, pp. 292–298.

Chen, T. Y., Huang, D. H., Zhou, Z. Q., 2006. Adaptive random testing through iterative partitioning. In: Proceedings of the 11th Ada-Europe International Conference on Reliable Software Technologies (Ada-Europe 2006). Vol. 4006 of Lecture Notes in Computer Science. Springer-Verlag, pp. 155–166.

Chen, T. Y., Kuo, F.-C., Liu, H., 2007a. Enhancing adaptive random testing in high dimensional input domains. In: Proceedings of 22nd Annual ACM Symposium on Applied Computing (SAC 2007). ACM Press, pp. 1467–1472.

Chen, T. Y., Kuo, F.-C., Liu, H., 2007b. Enhancing adaptive random testing through partitioning by edge and centre. In: Proceedings of the 18th Australian Software Engineering Conference (ASWEC 2007). IEEE Computer Society Press, pp. 265–273.

Chen, T. Y., Kuo, F.-C., Liu, H., 2007c. On test case distributions of adaptive random testing. In: Proceedings of the 19th International Conference on Software Engineering and Knowledge Engineering (SEKE 2007). pp. 141–144.

Chen, T. Y., Kuo, F.-C., Merkel, R., Ng, S. P., 2004b. Mirror adaptive random testing. Information and Software Technology 46 (15), 1001–1010.

Chen, T. Y., Kuo, F.-C., Zhou, Z. Q., 2007d. On favorable conditions for adaptive random testing. International Journal of Software Engineering and Knowledge Engineering 17 (6), 805–825.

Chen, T. Y., Leung, H., Mak, I. K., 2004c. Adaptive random testing. In: Proceedings of the 9th Asian Computing Science Conference. Vol. 3321 of Lecture Notes in Computer Science. pp. 320–329.

Chen, T. Y., Merkel, R., 2008. An upper bound on software testing effectiveness. Accepted to appear in ACM Transactions on Software Engineering and Methodology.

Ciupa, I., Leitner, A., Oriol, M., Meyer, B., 2006. Object distance and its application to adaptive random testing of object-oriented programs. In: Proceedings of the First International Workshop on Random Testing (RT06). Portland, ME, USA, pp. 55–63.

Ciupa, I., Leitner, A., Oriol, M., Meyer, B., 2008. ARTOO: adaptive random testing for object-oriented software. Accepted to appear in the 30th International Conference on Software Engineering (ICSE2008).

Finelli, G. B., 1991. NASA software failure characterization experiments. Reliability Engineering and System Safety 32 (1–2), 155–169.

Forrester, J. E., Miller, B. P., 2000. An empirical study of the robustness of Windows NT applications using random testing. In: Proceedings of the 4th USENIX Windows Systems Symposium. Seattle, pp. 59–68.

GCC, 2004. GNU compiler collection, `http://gcc.gnu.org`.

Hamlet, R., 2002. Random testing. In: Marciniak, J. (Ed.), Encyclopedia of Software Engineering, 2nd Edition. John Wiley & Sons.

Kuo, F.-C., 2006. On adaptive random testing. Ph.D. thesis, Faculty of Information and Communications Technologies, Swinburne University of Technology.

Laski, J. W., Korel, B., 1983. A data flow oriented program testing strategy. IEEE Transactions on Software Engineering 9 (3), 347–254.

Mayer, J., 2005. Lattice-based adaptive random testing. In: Proceedings of the 20th IEEE/ACM International Conference on Automated Software Engineering (ASE 2005). ACM, New York, USA, pp. 333–336.

Mayer, J., Schneckenburger, C., 2006. An empirical analysis and comparison of random testing techniques. In: Proceedings of the 2006 ACM/IEEE International Symposium on Empirical Software Engineering (ISESE 2006). ACM Press, pp. 105–114.

Merkel, R., 2005. Analysis and enhancements of adaptive random testing. Ph.D. thesis, School of Information Technology, Swinburne University of Technology.

Miller, B. P., Fredriksen, L., So, B., 1990. An empirical study of the reliability of UNIX utilities. Communications of the ACM 33 (12), 32–44.

Miller, B. P., Koski, D., Lee, C. P., Maganty, V., Murthy, R., Natarajan, A., Steidl, J., 1995. Fuzz revisited: A re-examination of the reliability of UNIX utilities and services. Tech. Rep. CS-TR-1995-1268, University of Wisconsin.

Myers, G. J., 2004. The Art of Software Testing, 2nd Edition. Wiley, New York.

Press, W. H., Flannery, B. P., Teukolsky, S. A., Vetterling, W. T., 1986. Numerical Recipes. Cambridge Unversity Press.

Regehr, J., 2005. Random testing of interrupt-driven software. In: Proceedings of the 5th ACM International Conference on Embedded Software (EMSOFT'05). New York, NY, USA, pp. 290–298.

Slutz, D., 1998. Massive stochastic testing of SQL. In: Proceedings of the 24th International Conference on Very Large Databases (VLDB 98). pp. 618–622.

White, L. J., Cohen, E. I., 1980. A domain strategy for computer program testing. IEEE Transactions on Software Engineering 6 (3), 247–257.

Yoshikawa, T., Shimura, K., Ozawa, T., 2003. Random program generator for Java JIT compiler test system. In: Proceedings of the 3rd International Conference on Quality Software (QSIC 2003). IEEE Computer Society Press, pp. 20–24.